224
7/22/79

dr. 2250

MASTER

MLM-2583

Proposed Implementation of Laser Raman Scattering Spectroscopy for Analysis of Hydrogen Isotopes

Stephen M. Craven and John T. Gill

February 14, 1979

Monsanto

MOUND FACILITY
Miamisburg, Ohio 45342

operated by
MONSANTO RESEARCH CORPORATION
a subsidiary of Monsanto Company

for the
U. S. DEPARTMENT OF ENERGY

Contract No. DE-AC04-76-DP00053

PRINTED IN THE UNITED STATES OF AMERICA

Available from
National Technical Information Service
U. S. Department of Commerce
5285 Port Royal Road
Springfield, Virginia 22161
Price: Printed Copy $4.00; Microfiche $3.00

MLM–2583
UC–4 and UC–37

Proposed Implementation of Laser Raman Scattering Spectroscopy for Analysis of Hydrogen Isotopes

Stephen M. Craven and John T. Gill

Issued: February 14, 1979

MOUND FACILITY
Miamisburg, Ohio 45342

operated by
MONSANTO RESEARCH CORPORATION
a subsidiary of Monsanto Company

for the
U. S. DEPARTMENT OF ENERGY

Contract No. DE-AC04-76-DP00053

Contents

Published by Information Services:
Roger E. Fitzharris, Editor

Abstract

Of the techniques described and investigated, coherent anti-Stokes Raman scattering (CARS) and laser Raman scattering (LRS) spectroscopies, the latter method proved to be more amenable to routine measurement of hydrogen isotopic species. It is shown that an available LRS instrument, with some improvements, could attain estimated relative standard deviation reproducibilities of 0.1 - 0.3% for major hydrogen components, an order of magnitude improvement over previously reported laser Raman analytical observations. Gases present at less than 0.1% of a sample could be observable with relative precisions as small as 2.4%. A system designed to obtain these results is proposed and discussed in detail.

Introduction

The goal of this work is to improve upon the accuracy of routine analytical technology [1] for analysis of hydrogen isotopic species. A precise and sensitive method is desirable. Several techniques have been considered. Recent emphasis has been placed on spectroscopic methods that will complement current mass spectroscopic capabilities. The hydrogen isotopic species produce infrared spectra only at pressures [2] too high for routine analytical work; it was thus desirable to consider optical techniques for which the selection rules predict activity for the hydrogen-hydrogen stretching mode. Two likely techniques are coherent anti-Stokes Raman spectroscopy (CARS) and laser Raman scattering spectroscopy (LRS). Results of experiments using these techniques are presented with appropriate background information. A proposal for the use of a laser Raman system for routine analysis of hydrogen isotopic species is also discussed.

Laser Raman Scattering Spectroscopy (LRS)

History

The Raman effect was discovered in 1928 by C. V. Raman in India [3] and Landsberg and Mandelstan [4] in Russia. This old technique has been used almost exclusively for determination of molecular spectroscopic parameters and molecular structure. Its use for the routine quantitative analysis of hydrogen isotopic species with results comparable to those of mass spectroscopy has been proposed [5] but not previously demonstrated. Some of the developments that have made quantitative analysis of gases possible are discussed here.

The earliest Raman work concerned liquids and solids; but, in 1929, Rasetti [6] reported the rotational Raman spectra of simple gases: N_2, O_2, and H_2. After the early interest, little was published in the field of Raman spectroscopy of gases during the years 1935 through 1951. This lack of activity resulted from one experimental problem: Raman scattering from gases is a weak effect. A resurgence of interest resulted in the early 1950's with the development of the high intensity mercury lamp called the "Toronto Lamp"[7]. Using the 4358Å line from this lamp, rotational Raman spectra of gases at moderate pressures could be photographed with spectrographs and exposure times of several hours. The vibration-rotation spectra required both higher pressures and longer exposure times. Most of the work during this period concerned the accurate measurement of vibrational frequencies for a number of molecules. Another innovation of this period was the use of reasonable quality photomultipliers.

The development that revolutionized the entire field of Raman spectroscopy was the use of the laser as a Raman excitation source [8]. The narrow line widths of lasers are particularly helpful in the study of gases, since the transitions under study are sharp. Furthermore, the high directional power available with laser sources permits the possibility of measurements using small gas volumes.

Two other developments have aided quantitative determinations by laser Raman scattering spectroscopy (LRS). To increase intensity-to-noise ratios of inherently weak signals, the use of photon counting detection was introduced in the late 1960's. In addition, in the mid-1970's, lasers were produced with electronic feedback mechanisms that permitted the laser power to be controlled to 0.5%.

In 1974, Setchell and Ottesen [5] first detailed the use of LRS for the quantitative analysis of hydrogen isotopes. Their experimental system made use of a very large light trapping cell designed by Hill and Hartley [9]. This multipass cell made the detection of small partial pressures possible. However the cell was of such a large volume, 24 liters, that it could not be used when only a limited amount of gas was available. The solution to this problem was suggested by Setchell and Ottesen and had been reported in 1972 by Kiefer et al. [10], who developed the external multipass illuminator shown in Figure 1. The sample cell has a volume of 3 cc. A gain factor of about 20 can be obtained with the multipass arrangement over a single-focused

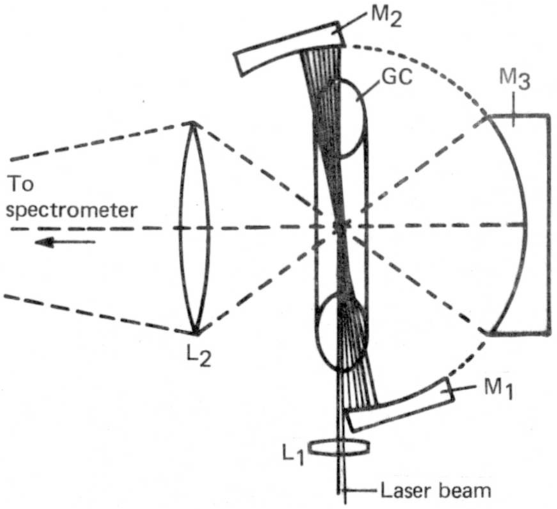

FIGURE 1 - Schematic of Raman multipass system. Spherical mirrors M_1, M_2 with radii of 4 cm and diameters of 2.5 cm, M_3 with a radius of 4 cm and a diameter of 5 cm. Lenses L_1, L_2 with a focal length of 5 cm. GC - gas cell.

laser beam. The limit of detection and signal reproducibility indicated by Setchell and Ottesen for their systems can now be extended to samples of limited size. Harney et al [11] have made use of similar instrumentation for the analysis of trace isotopic species in nitrogen and oxygen. The relative reproducibility of data obtained was 2-3% for species present at 0.4 to 0.8% of sample.

Raman intensities

The radiant intensity (power per unit solid angle) of the scattered Raman light for a particular transition is, by definition,

$$I_{RAMAN} = NV \frac{d\sigma}{d\Omega} I_{LASER}, \tag{1}$$

where N is the number of molecules per cm^3, $d\sigma/d\Omega$ is the differential Raman cross section, I_{LASER} is the laser beam irradiance (power/unit area), and V is the volume from which the scattered photons are observed. The Raman intensity for a particular transition is thus directly proportional to both laser power and concentration. Previous work [5] with hydrogen isotopes involved about 1 W of argon ion laser power at 4880Å. Today, 6 W of power are readily available (and even 15 W at considerable cost).

An important relationship exists between the differential Raman cross section and the frequency of the incident light, specifically:

$$\frac{d\sigma}{d\Omega} \propto \nu^4. \tag{2}$$

This means that incident radiation in the visible spectrum will give stronger Raman signals per incident photon than near infrared radiation and that ultraviolet radiation will give stronger signals than visible radiation. Thus, the detection limit for hydrogen isotopes could be extended by using a laser with output in the ultraviolet. Unfortunately, stable ultraviolet lasers are readily available with only about 1 W at 3638Å. Undoubtedly, higher-power ultraviolet lasers will be developed in the future.

Equation 1 predicts a linear relationship between Raman intensity and concentration. Quantitative measurements [12, 13, 14, 15] are made by measuring the Raman line intensities of the specie of interest at several known concentrations, thus describing a calibration plot. The Raman signal for an unknown amount of specie can then be measured, and observed precisions have been reported as low as ∿3% [14, 15].

Spectra of H_2 isotopic species

Two types of spectra can be observed by Raman spectroscopy for hydrogen (H_2), namely, the pure rotational spectrum and the vibration-rotation spectrum [16]. The pure rotational spectrum was observed in 1929, but no attempt to use this spectrum for quantitative analysis has been reported. The rotational spectrum is stronger than the vibration-rotation spectrum and may be useful for quantitative analysis of hydrogen isotopes under conditions of high resolution.

For this report, we are primarily interested in the vibration-rotation spectrum because of the wide separation between bands. Figure 2 is a composite of predicted Q-branch bands of the hydrogen isotopic species [5], assuming the wavelength of the incident laser light is 4880Å and

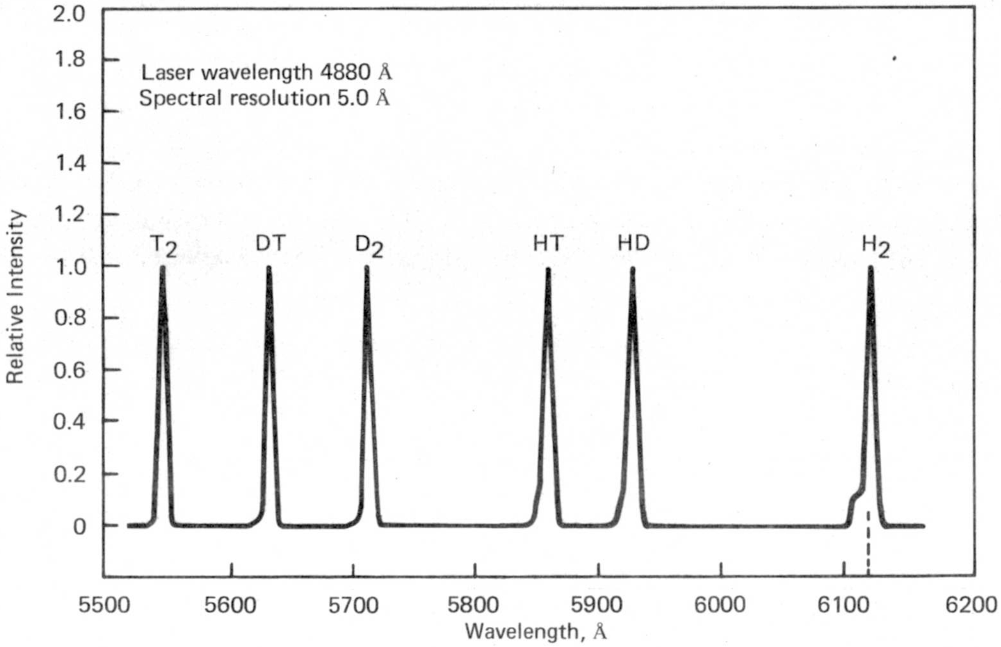

FIGURE 2 - Raman Q-branch bands of isotopic hydrogen molecules. D-deuterium, H-hydrogen, and T-tritium.

the spectral resolution is 5Å. S- and O-branch lines also exist, but these are weak compared to the Q-branch and are not shown in this figure. The minimum separation of ∿70Å (194 cm^{-1}) occurs between HT and HD. Such a separation is easily resolved with available spectrometers. The ease of spectral resolution of the Q-branch spectra of hydrogen species makes LRS very attractive for isotopic analysis. Although interference could arise from the bands of other molecules overlapping those of hydrogen in the mixture of interest, the percentage of impurity gases is often sufficiently small ($\leq 1\%$) that interference is not a problem.

Quantitative measurements for hydrogen isotopic species

As mentioned previously, Setchell and Ottesen [5] first proposed the use of LRS for quantitative analysis of hydrogen isotopic species. They predicted that the relative 3σ statistical error in measuring H_2 at a partial pressure of 38 torr corresponds to 0.285%. However, they did not extend their studies to mixtures containing all isotopic components; nor was their analysis based on a consideration of all system errors such as laser stability. But a similar proposal [11], based on somewhat more sophisticated instrumentation predicted an accuracy of 0.1% in the determination of hydrogen/deuterium isotopic ratios.

Coherent Anti-Stokes Raman Spectroscopy (CARS)

Coherent anti-Stokes Raman spectroscopy (CARS), one of a number of nonlinear

Raman processes that have developed in recent years with the availability of lasers, has been used by Regnier and Taran [17] to measure H_2 concentrations in N_2 from 10 to 10^6 ppm. Based on these and similar results [18, 19] the decision was made to investigate CARS as a technique for measuring hydrogen isotope concentrations.

Recently, an excellent review of CARS has appeared [20]. Using this technique, two relatively high-powered (typically pulsed) laser beams, at angular frequencies ω_1 and ω_s, are focused together in a sample. As a result of mixing the two lasers, a coherent Raman beam, which resembles a low-intensity laser beam at frequency $\omega_{as} = 2\omega_1 - \omega_s$, is generated in the medium. The efficiency of the conversion to frequency ω_{as} is critically dependent on: the presence of molecular resonances at a frequency $\omega_1 - \omega_s$, the laser intensities, the resonance line width, and the concentration. Since lasers can be spectrally narrowed to rather small widths with only small sacrifices in laser output, high resolution spectra are readily attainable.

The fundamental equation for CARS is:

$$P_{as} = \left(\frac{16\pi \ \lambda_s{}^4}{hc\lambda_\ell \lambda_{as}} \right)^2 \left[\frac{N\Delta i}{\Gamma} \left(\frac{d\sigma}{d\Omega} \right) \right]^2 P_\ell^2 P_s \qquad (3)$$

where P_{as} is the anti-Stokes power, N is the concentration of interacting molecules, Γ is the full width at half maximum of the Raman peak, Δ_i is the difference in population of the upper and lower states of the molecule, $d\sigma/d\Omega$ is the Raman differential cross section, P_l is the power of the pump beam, P_s is the power of the Stokes beam, and λ is the wavelength.

Significantly, P_{as} is proportional to the square of the pump power times the Stokes power. Variations in pump and Stokes power will severely affect the anti-Stokes power. Since fairly large peak-to-peak fluctuations (∿5%) exist in pulsed lasers today, CARS will have somewhat less precision than the theoretically simpler Raman scattering technique. In fact, Taran [18] has alluded to the difficulties with the reproducibility of CARS data. Average fluctuations in excess of 30% were observed--even in data corrected for laser power fluctuations by use of a reference. With improved mechanical stability, the fluctuation was reduced to 10%. Taran [18] notes that this figure is close to the error in reading output oscilloscope traces and corresponds to a 5% uncertainty in concentration.

Experimental

CARS

The CARS system used (Figure 3) was that of Prof. R. L. Byer of Stanford University. The pump beam was generated by a pulsed (10 pulses/sec) Nd:YAG laser with ∿5% peak-to-peak power stability. A coherent Stokes beam was obtained by passing a portion of the pump beam through a 1-meter long cell filled with 20 atm of H_2. Stokes and pump beams were focused inside a cell containing 0.1 to 10 atm H_2. The anti-Stokes output beam was filtered from Stokes and pump and monitored by a 1P28 photomultiplier tube with analog output to an oscilloscope.

LRS

The laser Raman system used was that of Spex Industries, Metuchen, New Jersey, where the results were obtained. Raman spectra were recorded from 4400 to 10 cm^{-1}

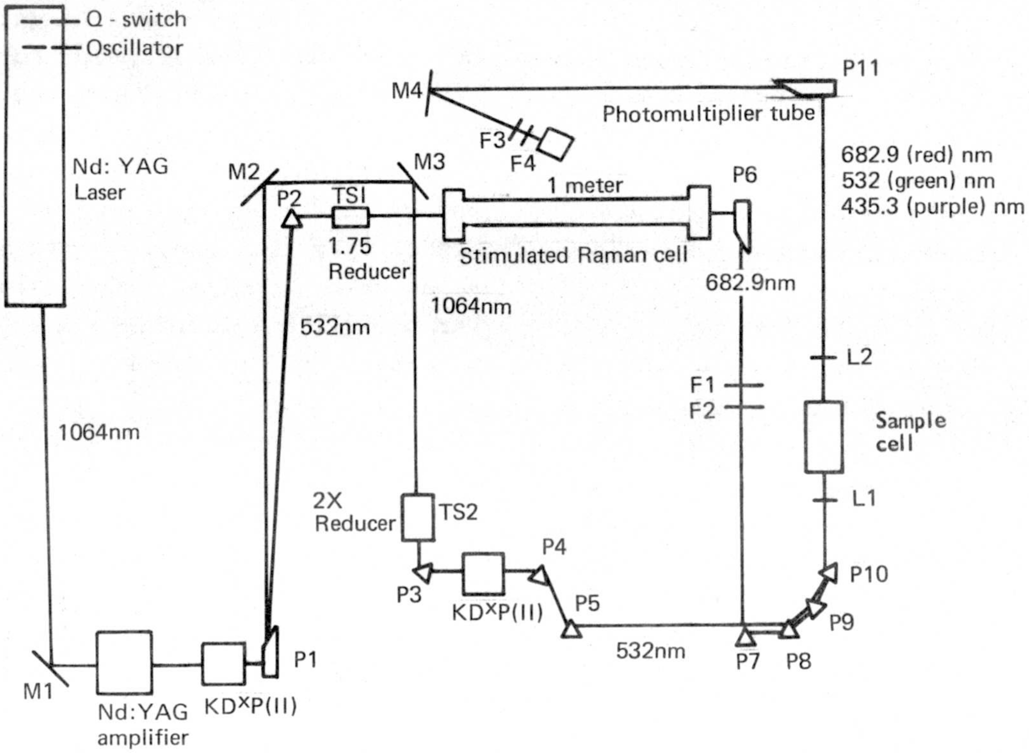

FIGURE 3 - Schematic of Stanford CARS system. M1-M4 minors, P1-P11 prisms, TS1 and TS2 beam reducing telescopes, F1-F4 filters, and L1 and L2 lenses.

with a Spex Ramalog instrument equipped with an argon-ion laser. The Ramalog is a double-monochromator instrument equipped with holographic gratings, and photon counting detection that used a cooled multi-alkali photomultiplier tube. Slit widths were 2.0 or 3.0 mm, producing smooth, unresolved observed band shapes from the hydrogen Q-branch rotational structures. The external resonating cavity and 3 cc volume gas cell permitted multipassing the 1.0 W 5145Å laser beam through the sample. Signal averaging was accomplished through the use of an Interdata computer interfaced to the Ramalog system; up to 20 peak scans were averaged. Integrated intensities were also obtained with the Interdata computer. The time required for one peak scan was 2-3 min and 20X signal averaging required about 60 min.

Results

CARS

The CARS results (Table 1) agree well with those of Taran [18] and show that the CARS signal increases as the square of the concentration as predicted by theory (Eq. 3). The slope of a log signal versus log pressure plot is about 2. Exact agreement is not obtained because of pressure broadening effects and the large errors in estimating the signal voltage. Signal variations of 30% or more were measured using the oscilloscope. Noise in a boxcar averaged signal from 10 atm of H_2 (time constant=1 sec) amounted to 15-20% of signal. As previously indicated, these errors were almost certainly caused by the peak-to-peak power fluctuations (∿5%) of the Nd:YAG laser. Such fluctuations make the use of a sophisticated reference

Table 1 - CARS RESPONSE SIGNAL VERSUS HYDROGEN GAS PRESSURE

Pressure (torr)	Signal (mV)
23 ± 2	3.0 ± 1.0
50 ± 2	10.0 ± 5
151 ± 2	70 ± 30
383 ± 2	350 ± 150
790 ± 2	1300 ± 500
7600 ± 2000	10000 ± 2000

system (double-beam instrument with standard gas) imperative for quantitative analysis.

The amount of signal available from H_2 at 0.1 atm was only barely detectable. Although this situation could be improved by more careful design, a reference system would surely decrease sensitivity. Another source of uncertainty in the CARS measurements is the drift in the CARS signal from the instability of the optical components. A decrease in the CARS signal of 25% was measured in less than 45 min. Detuning of the two KD*P(II) doubling crystals, the Nd:YAG laser, and a beam crossing prism were found to cause this error (probably as a result of room temperature instability). During operation, the laser power supply emanated sufficient heat to increase the room temperature 15-20°F. Frequent optimization of the prism, doublers, and laser were necessary.

In a routine production system, this type of behavior would be intolerable. A referencing system would further complicate instrumental ruggedness.

Because of the poor stability of the CARS system and the unliklihood of assembling a referenced system with even 1% reproducibility in signal, it was decided that an investigation of the LRS technique, which is theoretically and experimentally more straightforward, would be of value. Unfortunately, use of CARS for analytical work must await the arrival of stable pulsed lasers with smaller (<1%) peak-to-peak power fluctuations.

LRS

Data obtained using the LRS technique were more encouraging than CARS results for routine analytical purposes. Observations of within-half-day and between-day reproducibilities of individual hydrogen specie peaks, as well as some within-half-day precisions of signal averaged data, are given in Table 2. In general, these precisions approach the desired level of ∼1% relative standard deviation and apply to gases of partial pressures as low as 6 torr. Total instrumental response to H_2, HD, and D_2 from two different sample mixtures are included.

Depending on the particular sample and run, it can be seen that reproducibilities, listed as relative standard deviations, vary considerably. The magnitude of a peak in terms of total counts appears to affect reproducibility, in accord with implications of photon counting and Poisson statistics [21]. Thus, the effect of opening the width of the four monochromator slits from 2 to 3 mm, decreasing resolution but increasing the total throughput of photons, is to increase relative precision about 10-fold for the smallest sample. This effect is not that obvious for larger samples, where precision is determined more by overall instrumental stability than by uncertainties that arise from photon counting statistics. It would appear that system instability for the periods over which data were obtained was on the order of 1.5%

Table 2 - OBSERVED REPRODUCIBILITY OF HYDROGEN PEAK INTENSITIES BY LRS

Gas	Sample	Partial Pressure (torr)	Monochromator Slit Width (mm)	Time/Date	Av Total Counts Per Scan	No. of Independent Runs	No. of Scans Per Run[a]	$\frac{\sigma_o(I,w)}{I}$[b] (%)	$\frac{\sigma_o(I,B)}{I}$[c] (%)
H_2	B	6.21	2	P.M. 9/1/77	19,751	4	1	21.0	
H_2	B	6.21	3	P.M. 9/8/77	113,740	3	1,4,20	1.14	0.84
				A.M. 9/9/77	114,077	2	20	0.28	
H_2	A	28.13	3	P.M. 9/9/77	407,622	1	20		
HD	B	65.18	2	P.M. 9/1/77	207,222	5	1	1.06	
HD	B	65.18	3	P.M. 9/8/77	1,149,426	2	1	1.63	2.80
				A.M. 9/9/77	1,098,258	2	1	0.23	
HD	A	46.08	3	P.M. 9/9/77	659,878	1	20		
D_2	B	314.09	3	P.M. 9/8/77	6,613,090	3	1	0.57	2.50
				A.M. 9/9/77	6,326,798	2	1	0.37	
D_2	A	25.09	3	P.M. 9/9/77	470,576	2	20	0.02	

[a] Numbers greater than 1 denote signal averaging.

[b] Observed relative 1σ reproducibility within one-half day.

[c] Observed relative 1σ reproducibility between days.

within-half-day and 3% between-day, with considerable scatter. Signal averaging compensated for much of the system's instability, since reproducibilities of multiscan data within-half-day were 0.02 and 0.28% for samples of 25 and 6 torr, respectively.

Figure 4 displays the response of the LRS instrument, in millions of counts per peak, as a function of gas concentration. Two between-day data points per plot allow for rather poor definition of the predicted linear relationship. If for each plot a straight line is drawn constrained to pass through the origin, all lines will pass within 3σ uncertainty limits of LRS data (assuming an ∿5% between-day stability for the instrument is assigned). LRS data from sample A are consistently low, a probable result of either low machine response for that day or some leakage of sample A from its cell during the two week period between filling and LRS measurement. Data shown in Figure 4 begin to comprise calibration plots for the analytical use of the instrument. Calibrations must be made more certain, however, before LRS can truly perform the task of accurate hydrogen isotope analysis.

Discussion

Based upon the previously discussed results, more intensive study was devoted to the LRS technique. At present, the greater instrumental flexibility of LRS coupled with its theoretical simplicity make it a clear choice over CARS for hydrogen analyses. But even an LRS as sophisticated as the one previously described (See page 7) requires improvements. Consequently, the purpose of this section will be to demonstrate the

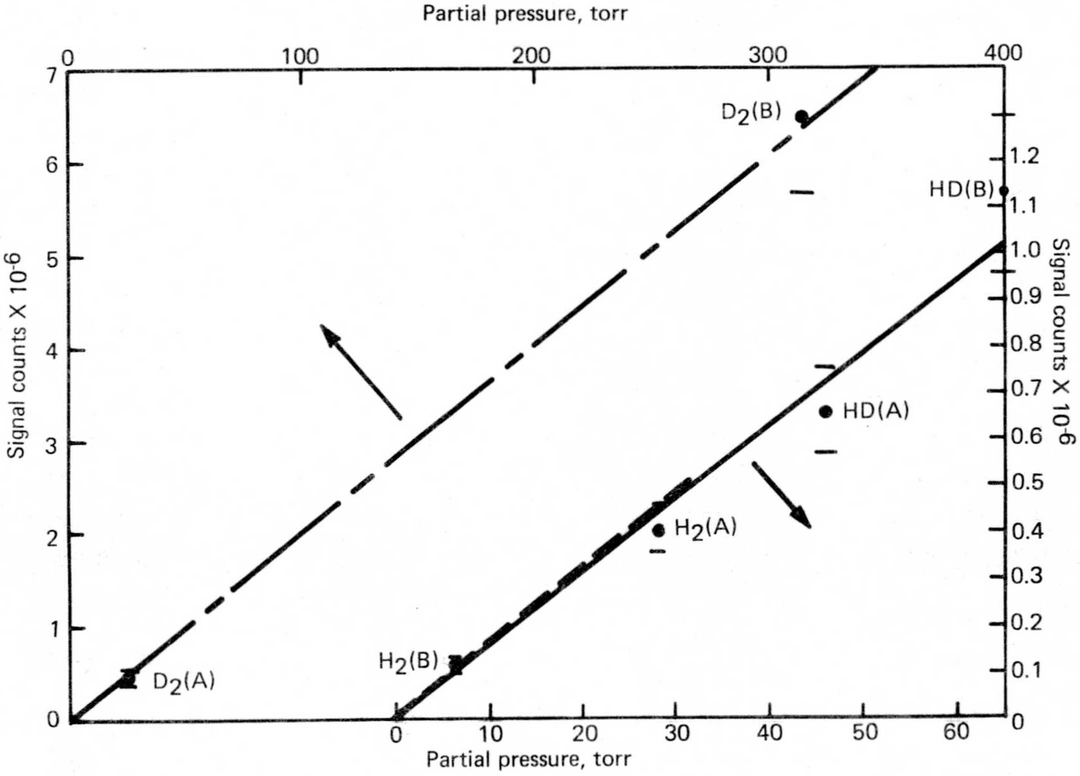

FIGURE 4 - Observed laser Raman signal versus partial pressure of three isotopic species of hydrogen.

theoretical precision limits of which the LRS is capable for hydrogen isotopic analyses using Spex instrumentation as a baseline (with successive improvements). A comparison to the hydrogen analyses of mass spectroscopy (Mound) will be made. Finally, the proposed in-house implementation of a high precision LRS system will be discussed.

Improvements and predictions

Much of the data obtained for this evaluation were limited in their precision by the stability of the system used, which was essentially determined by the laser itself. For the weakest peaks, however, reproducibilities were greatly affected by counting statistics because of small spectrometer light-throughput. Possible improvements in this system appear straightforward: increase throughput with a more powerful laser (thus bettering sensitivity) and increase the overall stability of the system, either with a steadier laser source or internal referencing.

The method of determining how these improvements should affect observed reproducibilities is based upon Poisson statistics [21]. (See page 9). Gas data are obtained on modern Raman spectrometers by individual photon counting. Since the absolute intensity of a Raman band is small, photon counting allows for the best attainable signal-to-noise ratios. Peaks such as those shown in Figure 2 may be readily integrated in a step-scan fashion: the spectrometer, under computer control, moves to a wave number setting on the baseline near a peak, the detection circuitry counts photons for a fixed time (for example, 1 sec), the total count is deposited in a computer register, and the spectrometer then moves on through the peak. An increment of one wave number is typical, with a total scan width of ∿180 wave numbers. Thus, the step-scan approaches a continuous integration of the peak shape, which is unsymmetrical because of the varying intensity of unresolved, rotational levels within the band. Integration of the full peak, as opposed to determination of peak amplitude, obviates considerations of temperature effects on rotational level populations, which could give rise to a slightly altered band shape.

Total gross peak intensity, I_G, is obtained by summing the stored counts for all intervals of the peak. Net intensity is determined by subtracting background from I_G,

$$I_N = I_G - I_B.$$

Background itself is assumed to contribute to I_G in a linearly varying fashion across the width of the peak. This "trapezoidal" background may be calculated from the counts observed at the first and last intervals of the scan, C_{B1} and C_{B2}, corrected for the total times spent measuring the gross peak and the two background levels, t_G, t_{B1}, and t_{B2}, respectively;

$$I_B = (C_{B1} + C_{B2}) \cdot [t_G/(t_{B1} + t_{B2})]. \quad (5)$$

The standard deviation of a photon-count intensity is known to vary as the square root of the total counts [21]. It can be readily shown [22] that the relative calculated uncertainty of a net peak intensity, based solely on counting statistics and assuming an infinitely stable instrument, may be expressed as:

$$\sigma_C(I)/I = \left[I_G + \left(\frac{t_G}{t_{B1}+t_{B2}} \right)^2 \cdot \left(C_{B1}+C_{B2} \right) \right]^{\frac{1}{2}} \Big/ I_N. \qquad (6)$$

Since no instrument is infinitely stable, however, another term must be added within the brackets of Eq. 6. Let ε represent the one sigma between-scan fractional stability of the instrument and n the number of scans involved in signal averaging. Then Eq. 6, with substitution from Eq. 5, becomes:

$$\sigma_C(I)/I = \left[I_G + \left(\frac{t_G}{t_{B1}+t_{B2}} \right) \cdot I_B + \frac{(\varepsilon I_N)^2}{n} \right]^{\frac{1}{2}} \Big/ I_N. \qquad (7)$$

This type of expression has been used previously to assign uncertainties to diffractometer photon-count x-ray data [23].

In terms of reproducibilities of intensity data, Eq. 7 predicts the results of modifying the instrument used in this study. Table 3 enumerates both observed (from Table 2) and calculated precisions for the system, as well as predicted reproducibilities for an instrument with various successive improvements. Values have been tabulated for samples actually studied, which represent a wide range in component concentrations. Calculated relative reproducibilities for the system used have incorporated the assumption that within-half-day stability of the instrument was 1.5%. Comparison of the first and second precision columns of Table 3 indicate that this is a reasonable estimate, though the spread in observed precision is rather broad. It may be noted that calculated precision for major components (above ∿30 torr) is indeed limited only by instrumental stability. Counting statistics affect more significantly the predicted reproducibilities of minor components. Perhaps the easiest way to surpass both statistical and stability limitations would be to incorporate a more powerful <u>and</u> stable laser, readily available with six times the power (at 5145Å) of the laser used, and with ±0.5% stability over an 8-hr period. Precisions attainable with such a system are predicted to improve two-to-threefold but are limited to 0.5% [column $\sigma_C{}^{i}(I,w)$, Table 3]. Signal averaging would be one method of minimizing uncertainty caused by random laser power fluctuations. An additional effect of 20X averaging [$\sigma_C{}^{ii}(I,w)/I$, Table 3], would be to improve predicted reproducibility (between sets of scans) by a factor of about $\sqrt{20}$. For the smallest of peaks, uncertainty in net peak intensity from a noisy background is substantial; but the uncertainty may be decreased by allotting more time to background determination. Measuring C_{B1} and C_{B2} each as an average of five counting intervals should increase background precision by a factor of $\sqrt{5}$, compared to a two-interval determination. This further decreases overall uncertainty of peaks, particularly for small components [$\sigma^{iii}(I,w)/I$, Table 3]. A fourth way to improve precisions would involve the additional installation of a laser power referencing system that would effectively hold laser power to ±0.1%. The results of such an improvement should follow those given in column $\sigma^{iv}(I,w)/I$ of Table 3. Precisions to 0.02% would be attainable for major components. Even without signal averaging, the remaining improvements yield relative reproducibilities of 0.1 to 0.2% for large peaks [$\sigma^{V}(I,w)/I$, Table 3].

Table 3 - PREDICTED REPRODUCIBILITY OF DATA FOR GASES SHOWN IN TABLE 2[a]

Gas	Sample	Partial Pressure (torr)	Monochromator Slit Width (mm)	$\frac{\sigma_o(I,w)}{I}$[b] (%)	$\frac{\sigma_c(I,w)}{I}$[c] (%)	$\frac{\sigma_c^{i}(I,w)}{I}$[d] (%)	$\frac{\sigma_c^{ii}(I,w)}{I}$[e] (%)	$\frac{\sigma_c^{iii}(I,w)}{I}$[f] (%)	$\frac{\sigma^{iv}(I,w)}{I}$[g] (%)	$\frac{\sigma^{v}(I,w)}{I}$[h] (%)
H_2	B	6.21	2	21.0	10.7	4.3	0.97	0.47	0.45	2.02
H_2	B	6.21	3	1.14	4.8	1.9	0.43	0.22	0.19	0.87
H_2	A	28.13	3	-	2.1	0.80	0.18	0.13	0.07	0.31
HD	B	65.18	2	1.06	1.9	0.72	0.16	0.12	0.06	0.27
HD	B	65.18	3	1.63	1.6	0.54	0.12	0.11	0.03	0.14
HD	A	46.08	3	-	1.7	0.63	0.14	0.12	0.05	0.20
D_2	B	314.09	3	0.57	1.5	0.50	0.11	0.11	0.02	0.10
D_2	A	25.09	3	-	1.9	0.67	0.15	0.12	0.05	0.24

[a] Based on the Spex Industries' laser spectroscopy system (Sept. 1977) with successive improvements.

[b] Observed relative 1σ reproducibility of signal within half-day; maximum value entered when applicable (from Table 2).

[c] Calculated relative 1σ reproducibility of signal within half-day, assuming a Spex Industries system: laser power = 1.000 ± 0.015 W, no signal averaging, two-point background calculation, no laser power referencing system.

[d] As in c, but laser power = 6.00 ± 0.03 W.

[e] As in d, but 20X signal averaging performed

[f] As in e, but 10-point background calculation performed.

[g] As in f, but referencing system implemented, effectively holding laser power to ±0.1% (indefinitely).

[h] As in g, but no signal averaging performed.

Data presented in Table 3 may be logically extended to gases at quite low concentrations. For H_2 at 0.5 torr, which would constitute 0.1% of a prospective sample, the predicted relative precision of the 20X signal-averaged peak on a fully improved system should be 2.4%. The potential sensitivity of the LRS technique is thus quite good for hydrogen analyses.

A comparison of the predictions of Table 3 to precisions obtainable through mass spectroscopy at Mound (MSM) is desirable. It must be noted that MSM tabulates accuracies for their data, which have been about twice the reproducibilities because of some peak overlaps and uncertain equilibrium calculations [25]. Since no overlap problems appear to exist in LRS, accuracies determined by this method should be nearly equal to reproducibilities. Also, accuracy estimates for hydrogen isotope mixtures have been reported by MSM for total isotope abundances [H], [D], and [T] [25]. Therefore, total isotope relative reproducibilities predicted for LRS and all its various improvements are calculated from Table 3; these relative reproducibilities are compared to relative MSM accuracies in Table 4. For a minor component, that is, 10% H, LRS results immediately approach those of MSM. However, for LRS to produce major component data of the quality obtainable through MSM, improvements to the Raman system are necessary. A good laser alone is not sufficient; either signal averaging or referencing are also needed, with the most versatile and time-efficient instrument incorporating both.

True accuracies in total isotope data from LRS will be somewhat in excess of reproducibility values given , by a contribution from the uncertainty in the components of calibrating mixtures (see page 20). Since the relative accuracies of major mixture components should be $\leq$0.1%, this factor will not greatly affect the comparisons of Table 4. In addition, the "dead time" of the individual photon counter [26] will cause major data peaks to be underestimated by a factor that is a function of counting rate. Although this factor will be used to correct such data, it will add an additional uncertainty (probably $\leq$0.1%) to major peak LRS results.

From the foregoing discussion, LRS holds great promise, both in precision and sensitivity, for the analyses of hydrogen isotope mixtures. Importantly, all of the suggested improvements to LRS instrumentation are feasible. The remainder of this report will thus deal with the properties and physical implementation of an LRS system, including improvements, at Mound. The preliminary design of such a system has been developed around that instrumentation used in the feasibility study.

Implementation of LRS at Mound

A proposed basic floor plan for a full LRS system is shown in Figure 5. The LRS spectrometer/computer instrument, the laser, gas delivery rack, and secondary containment plan are included in the full LRS system. All apparatuses should fit within a 10 by 15 ft area. The system as such would be dedicated to the analyses of hydrogen isotopic species. However other types of samples; gaseous, liquid, or solid, could be introduced for analyses following modifications of the sample compartment, gas rack, or glovebox.

Table 4 - COMPARISON OF REPRODUCIBILITIES OF LASER RAMAN DATA WITH ACCURACIES OF MOUND FACILITY MASS SPECTROSCOPY FOR SAMPLES OF DIFFERENT TOTAL ISOTOPE ABUNDANCES

			Mass Spectroscopy	Laser Raman Spectroscopy						
Isotope	Sample	Abundance (mole %)	$\frac{\sigma(A)}{A}$[a] (%)	$\frac{\sigma_O(A,w)}{A}$[b] (%)	$\frac{\sigma_C(A,w)}{A}$[c] (%)	$\frac{\sigma_C^{i}(A,w)}{A}$[d] (%)	$\frac{\sigma_C^{ii}(A,w)}{A}$[e] (%)	$\frac{\sigma^{iii}(A,w)}{A}$[f] (%)	$\frac{\sigma^{iv}(A,w)}{A}$[g] (%)	$\frac{\sigma^{v}(A,w)}{A}$[h] (%)
H	A	51.53	>0.4	-	1.39	0.52	0.12	0.09	0.04	0.19
H	B	10.06	1.60	1.38	1.55	0.55	0.12	0.10	0.04	0.18
D	A	48.47	0.28	-	1.28	0.46	0.10	0.08	0.04	0.16
D	B	89.94	0.19	0.54	1.37	0.46	0.10	0.10	0.02	0.09

[a] Relative 1σ accuracy of isotope abundance as determined by mass spectroscopy.

[b] Observed relative 1σ reproducibility (maximum) of isotope abundance within-half-day by laser Raman.

[c] Calculated relative 1σ reproducibility of isotope abundance within-half-day for laser Raman assuming unmodified Spex Industries system detailed in Table 3, footnote c.

[d] As in c, but see Table 3, footnote d.

[e] As in d, but see Table 3, footnote e.

[f] As in e, but see Table 3, footnote f.

[g] As in f, but see Table 3, footnote g.

[h] As in g, but see Table 3, footnote h.

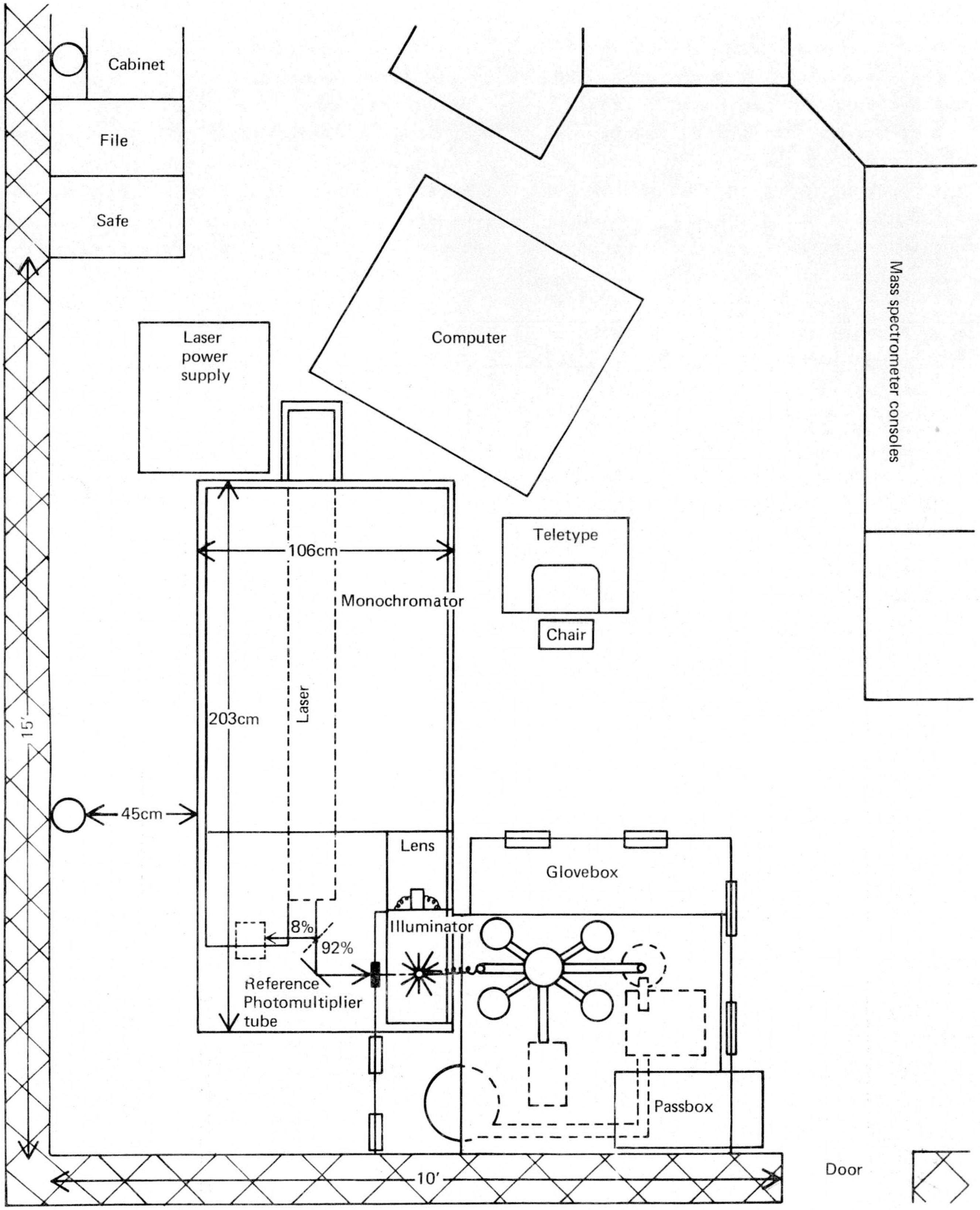

FIGURE 5 - Proposed floor plan for an LRS system (view from above).

In the proposed system, a 15-W multiline, argon-ion laser is used as the source. The 6-W line at 4880Å may be chosen over that at 5145Å , giving the user an ∿20% advantage in scattered Raman intensity and thereby increasing sensitivity somewhat beyond that which was previously discussed. About 4% of the laser beam is sampled by a glass slide, attenuated by neutral density filters, and measured by a reference photomultiplier tube in the photon counting mode. Counts from this reference train are accumulated in a digital photometer register. The main laser beam is directed through a quartz window in the glovebox and into the sample compartment by one or two mirrors. The beam enters a multipass cavity (Figure 1), at the center of which is located the sample cell. Scattered light from the sample gas is focused by lenses onto the entrance slit of the monochromator. Entrance, exit, and intermediate slits are opened full width (3 mm) for greatest light throughput attainable, at a spectral resolution of $\sim 35\ cm^{-1}$ (or ∿9Å for a 5145Å source) which is adequate for hydrogen samples. Adjustment of the monochromator to a desired wave number is accomplished manually or by computer. Step scans may be performed with a minimum drive step increment of $0.02\ cm^{-1}$. Resolved light exits the monochromator and impinges upon a cryogenically cooled gallium-arsenide photomultiplier tube, in photon counting mode with a dark background of <30 pps. Counts from this detector are accumulated in a second channel of the digital photometer. Sample data are transferred to the computer at the completion of each counting interval, determined by the accumulation of x counts (for example, 500,000) in the reference channel. The computer is used to collect and integrate data peaks automatically and signal average if necessary. If desired, the computer may be further programmed to control an entire data collection scheme whereby: peaks are scanned, standard deviations are assigned, decisions are made regarding signal averaging vis-a-vis time constraints, raw data are transformed to partial-pressure and mole-percent results based upon calibration curves stored within, and results are formatted for output to teletype or magnetic tape.

Secondary containment is critical to the application at hand. The glovebox shown in Figure 5 encloses a volume of approximately 100 ft^3. The glovebox contains gas handling rack and the sample illuminating compartment; the metal wall normally separating the latter from the spectrometer lens area forms a containment barrier in itself. However, between that wall and the adjustable lens holder, flexible bellows are needed. A passbox and gloveports are also shown in Figure 5. A metal table supports the main gas rack, below are: vacuum pumps, oil and gas storage volumes, and plumbing.

Figure 6 shows the proposed gas handling rack in detail. This rack is in closest possible proximity with the sample cell so as to minimize the amounts of gas required for sampling and calibration. A length of metal flex-tubing connects the sample cell to the rack, which affords some flexibility in orienting the cell properly. A slot is cut into the sliding sample compartment cover to eliminate interference from the flexible tubing. Outside the compartment, both temperature and pressure sensors monitor the sample gas. A constant temperature (H_2O) line coils about the rack in those areas critical to accurate measurement of gases. Unknown

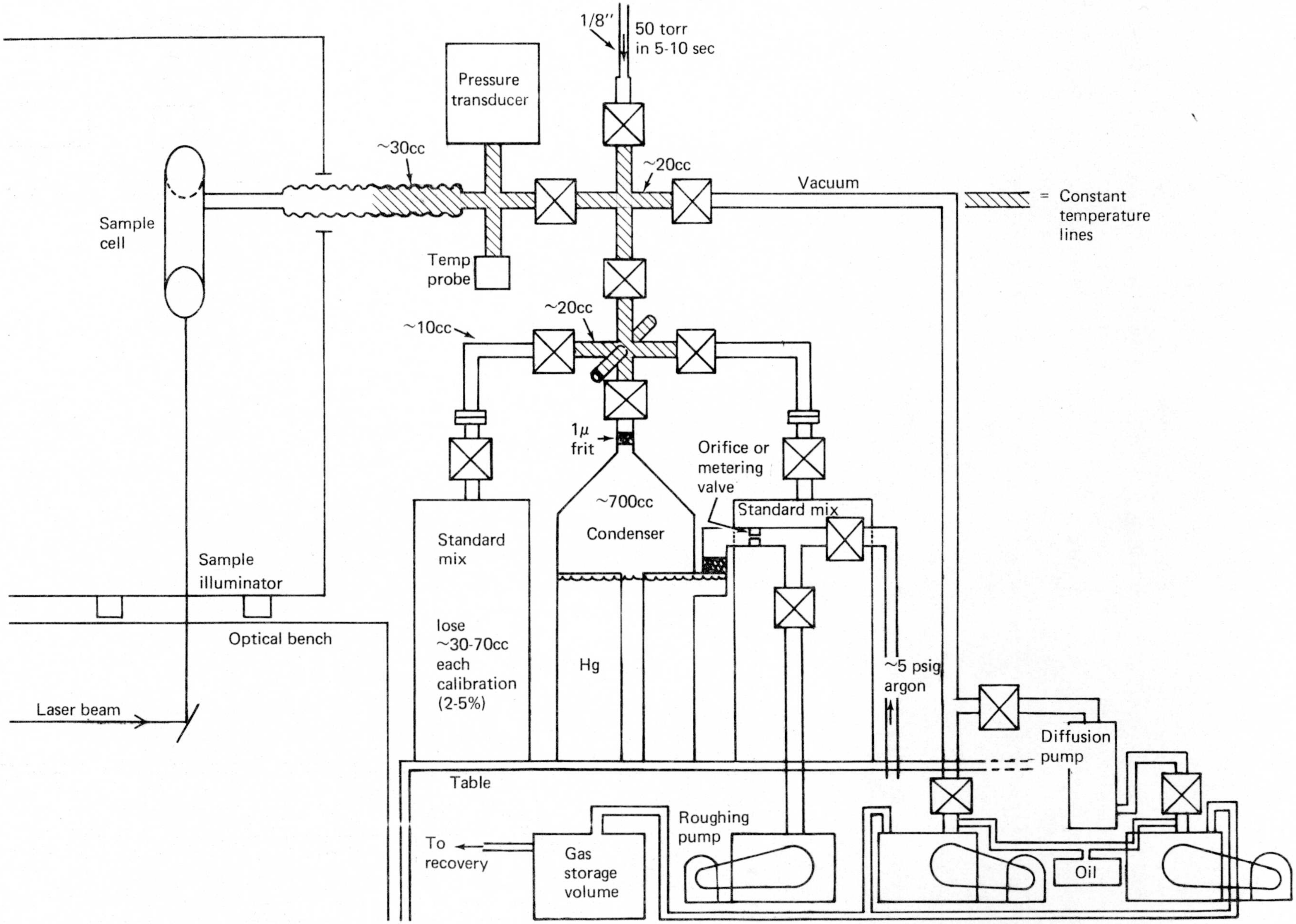

FIGURE 6 - Proposed gas handling rack for an LRS system (side view).

sample gases may enter the rack through the 0.125 in. line above the system; these unknown gases may then be compressed into the sampling volume by the condenser. The condenser is mercury-filled and operated by pressurized argon and vacuum lines connected to the lower condenser chamber. Given approximate volumes within the gas rack and computed flow rates [27], a one-liter external sample at atmospheric pressure will deliver enough gas through ∿100 ft of 0.125 in. line within 5-10 sec to fill the LRS cell to 500 torr pressure (following compression). Standard mixture gases may also be compressed into the LRS cell if necessary; in fact, much of a standard gas may be pumped back into its container were this deemed satisfactory. The "close-packing" arrangement of standard containers about the condenser minimizes waste of calibrating mixtures. Loss of standard should be between 2 and 5% with each use, depending on whether some of it is reclaimed. Vacuum and pressurized argon lines lead below the gas rack table. Both high and low vacuum are available to the gas rack. A volume is attached at the pump exhaust ports for the storage of recoverable gases. For containment of tritiated pump oils (for safe disposal) and rapid oil change, a pump oil storage volume is also located below. A separate low-vacuum pump is dedicated to the condenser. Gas rack valving may be either hand operated, remote air operated, or computer-controlled remote air operated. Initial testing of the rack would be easiest through manual operation. Later developments of the sampling method could include computer control of valving.

A discussion of LRS implementation at Mound is not complete without addressing the calibration requirements of such a system. Perhaps the simplest method is through determination of relative instrumental response to the six hydrogen diatomics (dependent on their different Raman cross sections). This allows for analysis of isotopic abundances within the hydrogen fraction of an unknown gas. However, the size of the hydrogen fraction compared to other gases present (for example, helium) could not be determined. An absolute calibration method, however, would yield results as actual partial pressures of hydrogen gases present. Knowledge of total sample pressure would thus allow computation of residual gases by subtraction. The absolute method is likely to be preferred and is discussed further.

Since only four standard mixture ports have been included in the gas rack design (Figures 5 and 6), and since these mixtures are quite expensive, one would like to use a limited number of standard gases for initial calibration. To produce an adequate amount of calibration data, the gas rack and condenser pump will be used to inlet aliquots of standard gases and adjust their pressures. Factors such as narrowing or broadening of line widths, and line frequency shifts as a function of pressure, are not expected to affect LRS results [28]. Total pressures of gases analyzed will be maintained below one atmosphere for safety reasons. The following approximate standard gases, premixed and stored at about 500 torr pressure, should suffice for calibration: (1) 25% H_2, 50% HD, 25% D_2; (2) 80% total D, 20% total T; (3) 20% total H, 80% total T; and (4) 99.99% D_2. The total pressure of gases aliquotted into the sample cell will be accurately measured, while constant temperature of the sample is maintained. For example, 100 torr of gas

(1) may be inlet to the evacuated sample cell. This pressure will be read to $\lesssim$0.02% (1σ) relative accuracy and the temperature to 0.1°C. With gas (1) components known to $\lesssim$0.05%, the sample component partial pressures should be known to $\lesssim$0.10% relative. The standard gas may be brought to a somewhat different total pressure by adjusting the condenser carefully. Raw count data obtained in LRS for various pressures of gas (1) will allow for calibration lines of instrumental response in total peak counts versus partial pressure for: the species (and approximate pressure ranges) H_2 (0 - 150 torr), HD (0 - 300 torr), and D_2 (0 - 150 torr). Data from gas (4) will produce a calibration for D_2 to $\sim$600 torr.

The diatomic compositions of gases (2) and (3), because of somewhat uncertain equilibrium constants, are unfortunately not known to 0.1% [29]. However, the total isotopic abundances in gases (2) and (3) should be accurate to $\leq$0.10% relative. Since instrumental response for D_2 will already be known from gas (1) and (4) data, $[D_2]$ in gas (2) will be experimentally obtainable. Because total [D] and [T] of gas (2) will be known, so then will be [DT] and $[T_2]$ in the mixture.

From these results, calibrations for DT (0 - 200 torr) and T_2 (0 - 25 torr) will be obtained. Similar use of gas (3) will yield calibrations for HT (0 - 200 torr) and T_2 (25 - 600 torr). Because of the propagation errors, relative uncertainty in calibrations of low pressure components may reach several percent. To decrease this value, use of additional standard mixtures may be necessary. Alternative calibrations for HT and DT might be derivable from a theoretical determination of relative Raman cross sections of hydrogen isotope diatomics [30]. This would, however, be a laborious task, the results of which might still have to be corroborated experimentally.

Following the task of initial calibration of the LRS instrument, periodic checks of system response will be necessary. These recalibrations, which will be required daily or perhaps weekly, will monitor changes in the alignment of the optics and in spectrometer throughput for the various hydrogen species. The method should be simple: analyze peak intensities day-to-day from the standard gas (1) (sample cell of course always filled to the same pressure). From variations in peak intensities one will calculate normalization factors, NF, to be applied to the data of that day n. If NF_n (H_2), NF_n (HD), and NF_n (D_2) are non-unity, yet are nearly identical (within confidence limits), sample illumination alone will have changed somewhat; and the effect on all data will be equal. Thus the average NF_n will be applied to all day n-data, which includes that of HT, DT, and T_2. Were the three observed factors significantly different, however, the sensitivity of the spectrometer to each molecule will have changed independently, (altered optical alignment or dust collected on the gratings might conceivably cause this). Each NF_n will have to be applied to its particular specie, and additional factors for HT, DT, and T_2 will be necessary. A second standard gas will have to be analyzed. Individual changes in instrument sensitivity are, however, less likely than a single overall change. Daily recalibration (or weekly, if the instrument proves more durable) should not, therefore, be inordinately time consuming.

Conclusion

Observed results and extensive calculations indicate that laser Raman scattering spectroscopy (LRS) is a technique that will be complementary to mass spectroscopy in the analysis of hydrogen isotopes. LRS will provide data on the absolute partial pressures of hydrogen diatomics in an unknown, with precisions to an estimated relative standard deviation of 0.1 - 0.2%. This will be an order of magnitude improvement over previously reported laser Raman analytical observations. Also measurement of other molecular gases such as N_2 is entirely possible. The amount of monatomic inert gases present in a sample, though these are invisible to LRS per se, may be determined by subtraction of known component partial pressures from the total sample pressure.

It has been shown that an LRS system could be implemented at Mound with relative ease. The design, calibration, and handling of such an instrument have been projected in some detail, and a more detailed design and cost accounting of the overall system is in preparation.

LRS is a very versatile technique since readily modified forms of the LRS system (primarily in sample compartment) could probe liquids, solids, and surfaces, as well as gases, with considerable accuracy. The compositions of solid hydrides, interactions of pollutant molecules with catalytic surfaces, adsorption of hydrogen on metals, organic components of oil-bearing shales in situ, and analysis of polyatomic anions [12,13] and organics [14] in aqueous solutions might all conceivably be investigated. Processes as difficult to monitor as the combustion of fuel gases in an engine have already been studied with further modified LRS sampling and detection systems [31,32]. Furthermore, the addition of an optical multichannel analyzer could allow the investigation of time-resolved explosion chemistries and temperatures.

Acknowledgements

The authors would like to thank Prof. Robert L. Byer for helpful discussions and the use of his laboratory for CARS experimentation; Spex Industries for providing LRS data and ideas for improving their instrumentation; R. W. Baker, P. D. Bantz, and J. C. Miles for their valuable discussions concerning gas handling and calibration of an LRS system; R. E. Ellefson for his many helpful comments in reviewing this manuscript; and J. C. Birkbeck for her help in proofreading.

References

1. A. Attalla, C. T. Bishop, D. R. Bohl, T. L. Buxton, R. E. Sprague, and D. K. Warner, Assessment of Methods for Analyzing Gaseous Mixtures of Hydrogen Isotopes and Helium, MLM-2376 (Oct. 20, 1976), 14 pp.

2. R. D. G. Prasad and S. Paddi Reddy, J. Chem. Phys., 65, 83 (1976); S. Paddi Reddy and K. S. Chang, J. Mol. Spectrosc., 47, 22 (1973).

3. C. V. Raman, Indian J. Phys., 2, 287 (1928).

4. G. Landsberg and L. Mandelstan, Naturwissenschaften, 16, 557, 772 (1928).

5. R. E. Setchell and D. K. Ottesen, The Potential Use of Raman Spectroscopy in the Quantitative Analysis of Hydrogen Isotopes, SAND-74-8644, Sandia Laboratories, Livermore, Livermore, Calif. (February 1975).

6. F. Rasetti, Proc. Natl. Acad. Sci. Am. 15, 515 (1929); Phys. Rev., 34, 367 (1929).

7. H. L. Welsh, M. F. Crawford, R. T. Thomas, and G. R. Love, Can. J. Phys., 30, 577 (1952).

8. S. P. S. Porto and D. L. Wood, J. Opt. Soc. Am., 53, 1446 (1962).

9. R. A. Hill and D. L. Hartley, Appl. Op., 13, 186 (1974).

10. W. Kiefer, H. J. Bernstein, H. Wieser and M. Danyluk, J. Mol. Spectrosc., 43, 393 (1972).

11. R. C. Harney, S. D. Bloom, and F. P. Milanovitch, Stable Isotope Ratio Measurements in Hydrogen, Nitrogen, and Oxygen Using Raman Scattering, UCRL-76743 (CONF-750806-3), Lawrence Livermore Laboratory, Livermore, Calif. (Aug. 6, 1975).

12. D. E. Irish and H. Chen, Appl. Spectrosc., 25, 1 (1971); D. E. Irish and J. D. Riddell, Appl. Spectrosc., 28, 481 (1974).

13. A. L. Marston, Nucl. Technol., 25, 576 (1975); A. G. Miller, Anal. Chem., 49, 2044 (1977).

14. D. M. Thomas, Appl. Spectrosc., 31, 515 (1977).

15. W. F. Adolfson, R. G. Schlecht, and J. B. Morton, Appl. Phys., 14, 49 (1977).

16. G. Herzberg, Molecular Spectra and Molecular Structure, Vol 1: "Spectra of Diatomic Molecules," van Nostrand Co., Princeton, New Jersey, 1963, p. 61.

17. P. Regnier and J. P. E. Taran, Appl. Phys. Lett., 23, 240 (1973).

18. J. P. E. Taran in Tunable Lasers and Applications, A. Mooradian, T. Jaeger and P. Stokseth (eds.), Springer-Verlag, New York, 1976, p. 378.

19. J. W. Nibler, J. R. McDonald and A. B. Harvey, Opt. Commun., 18, 371 (1976).

20. W. M. Tolles, J. W. Nibler, J. R. McDonald, and A. B. Harvey, Appl. Spectrosc., 31, 253 (1977).

21. P. R. Bevington, Data Reduction and Error Analysis for the Physical Sciences, McGraw-Hill Co., New York, 1969, pp. 36-42.

22. Ibid., pp. 56-62.

23. W. R. Busing and H. A. Levy, J. Chem. Phys., 26, 563 (1957).

24. P. W. R. Corfield, R. J. Doedens, and J. A. Ibers, Inorg. Chem., 6, 197 (1967).

25. Technical Manual PD 80026, Mound Facility Standard Analytical Procedures, Operation 192.

26. J. M. Hayes, D. E. Matthews, and D. A. Schoeller, Anal. Chem., 50, 25 (1978).

27. S. Dushman, Scientific Foundations of Vacuum Technique (2nd ed.), John Wiley and Sons, Inc., New York, 1962, p. 82.

28. V. G. Cooper, A. D. May, E. H. Hara, and H. F. P. Knapp, Can. J. Phys., 46, 2019 (1968); V. G. Cooper, A. D. May, and B. K. Gupta, Can. J. Phys., 48, 725 (1970); P. Dion and A. D. May, Can. J. Phys., 51, 36 (1973).

29. W. M. Jones, J. Chem. Phys., 17, 1062 (1949).

30. T. C. James and W. Klemperer, J. Chem. Phys., 31, 130 (1959); H. A. Hyatt, J. M. Cherlow, W. R. Fenner, and S. P. S. Porto, J. Opt. Soc. Am., 63, 1604 (1973).

31. R. E. Setchell and D. P. Aeschliman, Appl. Spectrosc., 31, 530 (1977).

32. M. Lapp, Laser Raman Gas Diagnostics, M. Lapp and C. M. Penny (eds.), Plenum Press, New York, 1974, p. 107.

Distribution

EXTERNAL
Technical Information Center, UC-4 and 37 (232)
Technical Report Library, Monsanto, St. Louis

R. K. Flitcraft, Monsanto Research Corporation
R. C. Harney, Massachusetts Institute of Technology
C. M. Hartwig, Sandia Laboratories, Livermore
H. N Hill, DOE/ Dayton Area Office
R. E. Meirs, Purdue University
W. E. Moddeman, University of Dayton
R. E. Setchell, Sandia Laboratories, Albuquerque
C. P. Sutter/R. N. Diebel, Atlantic Richfield Hanford Company
J. Umbarger, Los Alamos Scientific Laboratory
D. White, University of Pennsylvania

INTERNAL
Library (15)
Publications

W. R. Amos
T. L. Buxton
W. T. Cave
S. M. Craven
V. M. Franchetti
J. T. Gill
J. P. Highland
C. W. Huntington
C. J. Kershner
B. R. Kokenge
J. R. McClain
D. R. Spangler
R. E. Vallee
H. A. Woltermann